Analysis of Capillary Guided Laser Plasma Accelerator Experiments at LBNL

K. Nakamura[*†], A. J. Gonsalves[*], D. Panasenko[*], C. Lin[*‡], Cs. Tóth[*], C. G. R. Geddes[*], C. B. Schroeder[*], E. Esarey[*†] and W. P. Leemans[*†]

[*]*Lawrence Berkeley National Laboratory, University of California, Berkeley, CA 94720, USA*
[†]*University of Nevada, Reno, Reno, NV 89557, USA*
[‡]*Peking University, Beijing 100871, China*

Abstract. Laser wakefield acceleration experiments were carried out by using a hydrogen-filled capillary discharge waveguide. For a 15 mm long, 200 μm diameter capillary, quasi-monoenergetic e-beams up to 300 MeV were observed. By de-tuning discharge delay from optimum guiding performance, self-trapping was found to be stabilized. For a 33 mm long, 300 μm capillary, a parameter regime with high energy electron beams, up to 1 GeV, was found. In this regime, the electron beam peak energy was correlated with the amount of trapped electrons.

INTRODUCTION

Electron accelerators based on laser-driven plasma wakefield acceleration (LWFA) [1] have demonstrated high field gradients up to hundreds of GV/m, and the production of quasi-monoenergetic electron beams (e-beams) with energies of the order of 100 MeV in just a few millimeters [2–4]. Recently, by using a hydrogen-filled capillary discharge waveguide, LWFA up to a GeV has been realized at Lawrence Berkeley National Laboratory (LBNL) [5, 6]. In this scheme, intense laser pulses were guided over a distance 10 times the Rayleigh range by a preformed plasma channel with sufficiently low density to reduce energy gain limitations imposed by diffraction and dephasing [1]. During the laser plasma interaction, electrons were self-trapped from the background plasma, and accelerated up to the GeV level.

In the first generation of the capillary discharge guided LWFA experiments, accelerator performance was found to be quite sensitive and to exhibit a complicated interdependence on input laser and plasma parameters, such as the delay between the onset of the discharge current and arrival of the laser beam (discharge delay t_d), the estimated on-axis plasma density n_0 [7], the peak laser power P, and the capillary diameter. Electron beams with energies of 1 GeV were obtained in a 33 mm long, 300 μm diameter capillary for $P \sim 42$ TW and $n_0 \simeq 4.3 \times 10^{18}$ cm^{-3}. Although 1 GeV beam generation was not stable, a statistical analysis did show a parameter regime where 0.5 GeV e-beams were produced with improved stability by tightly controlling the input parameters for a 33 mm long, 225 μm diameter capillary.

In order to design the next generation apparatus for stable production of higher quality e-beams, with small emittance and high energy and charge, it is critical to untangle this interdependence of input laser and plasma parameters, which requires further parameter

CP1086, *Advanced Accelerator Concepts: 13th Workshop,* edited by C. B. Schroeder, W. Leemans, and E. Esarey

exploration and analysis. In this paper, we report a performance analysis of the capillary discharge guided LWFA using a 15 mm long, 200 μm diameter and a 33 mm long, 300 μm diameter capillary. Experiments varying capillary length give insight into the trapping and dephasing physics of the capillary discharge guided LWFA.

EXPERIMENTAL SETUP

The schematic of the capillary discharge guided LWFA experiments is shown in Fig. 1. The laser that was utilized was the short pulse, high peak power and high repetition rate (10 Hz) Ti:Al_2O_3 laser system of the LOASIS facility at LBNL. The laser was focused onto the entrance of a capillary discharge waveguide by an f/25 off-axis parabolic mirror. A typical focal spot size was $r_0 \simeq 25$ μm containing 60% of the laser energy. Here, a Gaussian transverse profile of $I = I_0 \exp(-2r^2/r_0^2)$ is assumed. Full energy and optimum compression gives $P = 43$ TW [$\tau_{in} \simeq 40$ fs in full width half maximum (FWHM) intensity], calculated peak intensity $I_0 = 2P/\pi r_0^2 \simeq 2.6 \times 10^{18}$ W/cm^2, and normalized vector potential $a_0 \simeq 8.6 \times 10^{-10} \lambda[\mu\text{m}] I^{1/2}[\text{W/cm}^2] \simeq 1.1$.

The capillary waveguide was laser-machined in a sapphire plate. Hydrogen gas was introduced into the capillary using two gas slots as shown in Fig. 1 (inset). A discharge was struck between two electrodes located at each end of the waveguide, using a high voltage pulsed power supply that utilized a 4 nF capacitor charged to between 15 and 18 kV. Measurements showed that a fully ionized, approximately parabolic channel was formed on axis [7]. This fully ionized feature was also confirmed by the absence of ionization induced blueshifting of the transmitted laser spectrum when a low power (< 0.2 TW) laser pulse was guided.

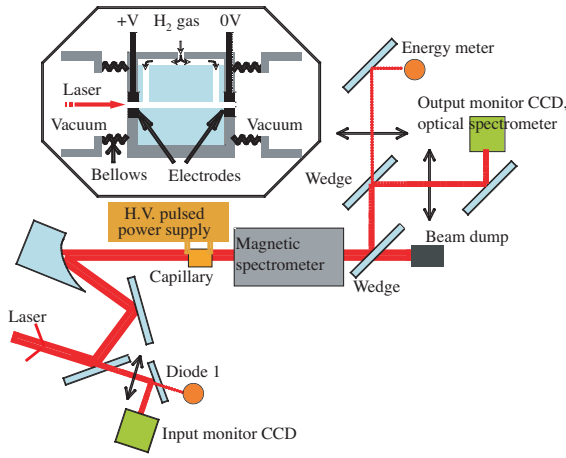

FIGURE 1. Schematic diagram of the capillary discharge-guided laser wakefield accelerator and diagnostics. The detailed description of the capillary discharge unit is in the upper inset, and that of the electron spectrometer can be found in Ref. [8].

The e-beams generated were characterized by an electron spectrometer utilizing a round dipole magnet with a maximum magnetic field of 1.25 T and effective radius of 195 mm. The magnetic spectrometer allowed simultaneous measurement of the laser and e-beam due to its large gap, and single shot measurement of electrons from 0.01 GeV to 0.14 GeV (bottom view) and 0.17 GeV to 1.1 GeV (forward view) [8]. The laser energy was monitored both before and after the interaction to evaluate the guiding efficiency and guided beam quality. The laser output spectrum was measured by a broadband optical spectrometer which covers a wavelength range of 320 to 1000 nm in a single shot.

RESULTS

In experiments using a 15 mm long, 200 μm diameter capillary, the guiding performance and e-beam generation showed clear dependence on the discharge delay. Shown in Fig. 2(a) are the discharge delay dependence of several binned spectra. The center is defined as the light within the frequency bandwidth of $770 \leq \lambda \leq 835$ nm, and 100% of incident light was within this band. The red (blue) shift is defined as $835 < \lambda < 1100$ nm ($320 < \lambda < 770$ nm). The input laser parameters were 0.9 J ($\pm$3%), 41 fs ($a_0 \sim 0.8$), and the plasma density was 2.5 or 3.7 $\times 10^{18}$ cm^{-3}. For relatively short discharge delay ($t_d <$ 130 ns), significant red-shift and moderate blue-shift were observed, consistent with the laser pulse modulation and energy deposition onto the plasma via wakefield generation. For longer discharge delay ($t_d > 130$ ns), optical spectrum exhibited significant blue-shift as well as red-shift, and the transmission efficiency dropped.

The probability of observing any e-beams on the electron spectrometer in the range from 0.01 to 1.1 GeV is shown in Fig. 2(b) by dashed lines. For $n_0 \sim 2.5 \times 10^{18}$ cm^{-3}, no electron beams were observed for $t_d < 110$ ns and transmission efficiency was high

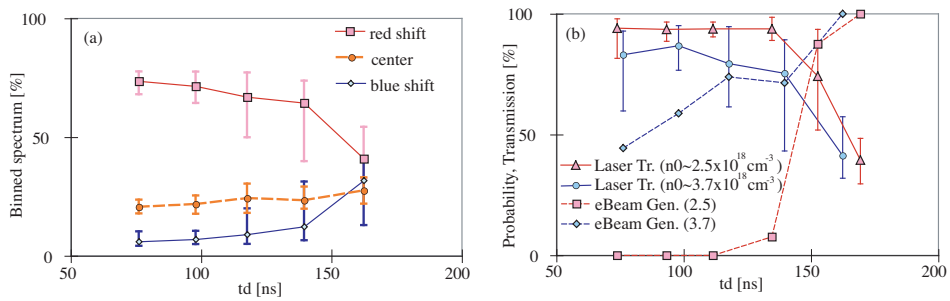

FIGURE 2. Results for 15 mm long, 200 μm diameter capillary: (a) Binned transmitted optical spectrum versus discharge delay for $n_0 \sim 2.5 \times 10^{18}$ cm^{-3}. The center is defined as the light within the frequency bandwidth of $770 \leq \lambda \leq 835$ nm. The red (blue) shift is defined as $835 < \lambda < 1000$ nm ($320 < \lambda < 770$ nm). (b) Transmission efficiency of laser pulses [solid line, triangles (circles) for $n_0 \sim 2.5(3.7) \times 10^{18}$ cm^{-3}], and the probability of e-beam observation on the electron spectrometer [dashed line, squares (diamonds) for $n_0 \sim 2.5(3.7) \times 10^{18}$ cm^{-3}] versus discharge delay. For both figures, the input laser parameters were 0.9 J ($\pm$3%), 41 fs ($a_0 \sim 0.8$). A total of 80 shots were taken for each plasma density. Bars show minimum and maximum points.

($>$ 80%). This suggests that, although a wakefield was generated based on the observation of significant red-shift, it was not large enough to trap background electrons. Electron beams were observed for longer discharge delay, along with a drop in transmission efficiency and enhanced blue-shift. Note that by using higher density plasma ($n_0 \sim 3.7 \times 10^{18}$ cm^{-3}), e-beams were observed for shorter discharge delay without significant blue shift in transmitted optical spectrum.

The peak of the e-beam energy distribution (peak energy), the highest energy of the e-beam energy distribution (maximum energy), and total charge observed on the spectrometer versus discharge delay for $n_0 \sim 3.7 \times 10^{18}$ cm^{-3} are shown in Fig. 3. One can see that relatively high energy, low charge e-beams were observed with shorter discharge delay while low energy, high charge beams were observed with longer delay. For longer discharge delay, electron beams occasionally exhibit broadband, multiple peak structure, and significant low energy tail.

Several mechanisms could be responsible for the enhancement of the blueshifting, laser transmission loss, and electron trapping observed for longer discharge delay. For longer discharge delay, the degree of ionization, depth of the plasma channel, and plasma density decrease. It has also been suggested that the amount of discharge-ablated material interacting with the laser pulse increased [9]. For a substantial amount of laser pulse energy to be blueshifted by ionization requires the peak intensity of the laser pulse to be within an order of magnitude of the ionization intensity of the ion species with which the pulse interacts. In the case of hydrogen this is 10^{14}–10^{15} W/cm^2, several orders of magnitude lower than the intensity of the laser in the channel. Ablated materials (e.g., aluminum, oxygen) have higher ionization thresholds, and the deteriorated channel may lead to laser ablation of the capillary wall. Alternatively, the blueshifting could be caused by photon acceleration of the back of the laser pulse [11], if it has stretched to a length of order the plasma wavelength. The reduced laser transmission was likely due to ionization and laser leakage from the channel rather than the stronger wakefield generation because of the lower maximum energy observed for longer discharge delay. For enhanced trapping, recent studies suggested the interaction with a partially ionized plasma could assist self-trapping [10, 12]. The discharge-ablated materials drifting to

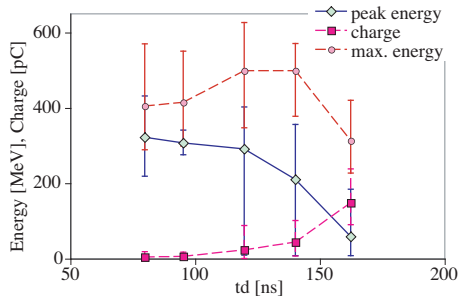

FIGURE 3. The peak energy (diamonds), maximum energy (circles), and total charge (squares) versus discharge delay for 15 mm long, 200 μm diameter capillary. Plasma density was $n_0 \sim 3.7 \times 10^{18}$ cm^{-3}, and the laser parameters were 0.9 J ($\pm$3%), 41 fs ($a_0 \sim 0.8$). A total of 54 shots were observed with electron beam. Bars show minimum and maximum points.

the axis before the arrival of the laser could contribute to this process. Note that the laser-ablated materials could not contribute to this process. Another possible reason is increase of the on-axis plasma density due to the deterioration of the channel. Although the degree of ionization decreases for longer discharge delay, the laser pulse was strong enough to ionize hydrogen.

In 2006, generation of e-beams with energies of 1 GeV was reported for a 33 mm long, 300 μm diameter capillary with three gas slots [5, 6]. Similar to these results, a parameter regime where e-beams with energies of up to 1 GeV were produced was found for a 33 mm long, 300 μm diameter capillary with two gas slots. Representative single shot e-beam spectra are shown in Fig. 4. The plasma density was $n_0 \sim 5.3 \times 10^{18}$ cm^{-3}, the laser parameters were 1.5 J ($\pm$5.7%), 46 fs ($a_0 \sim 0.93$), and the discharge delay was $t_d \sim 580$ ns. In this parameter regime, 51 shots were taken, and 37 shots produced electrons above 400 MeV. Average peak energy was 713 MeV, and average charge was 6 pC. Since e-beams were often observed with low energy tail in this regime, electronss with energy above 400 MeV were taken into account for the analysis. The average laser transmission efficiency was 65%. With this capillary, up to 70% transmission efficiency was observed for 700 ns discharge delay.

The peak energy and maximum energy versus total charge for 33 mm long, 300 μm diameter capillary are shown in Fig. 5. The peak energy showed clear dependence on the charge, while the maximum energy was somewhat insensitive to charge. One possible explanation of this observation is the beam loading effect. The trapped electron beam produces a wakefield which cancels the wakefield generated by the laser pulse. As a result, the tail of the electron beam sees lower accelerating field while the head sees maximum field, introducing energy spread to the electron beams. Another possible explanation is that the higher charge beams were trapped over a large phase region in the plasma wave, resulting in a larger energy spread. To produce e-beams in a reproducible manner, controlling the amount and the location of trapped electrons will be critical.

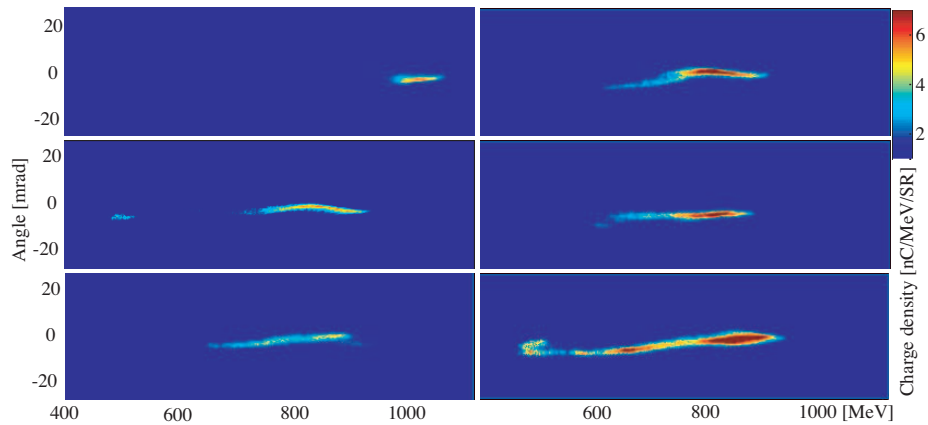

FIGURE 4. Representative single shot e-beam spectra for a 33 mm long, 300 μm diameter capillary. The density was $n_0 \sim 5.3 \times 10^{18}$ cm^{-3}, and the laser parameters were 1.5 J ($\pm$5.7%), 46 fs ($a_0 \sim 0.8$).

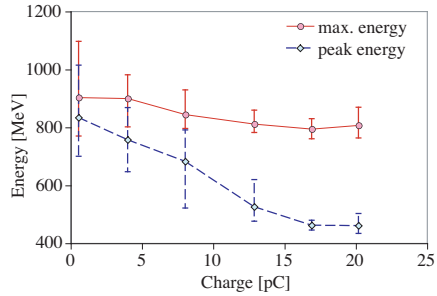

FIGURE 5. The peak and maximum energy versus charge for 33 mm long, 300 μm diameter capillary. Of a set of 51 shots, 37 shots had $>$ 400 MeV electrons. Bars show minimum and maximum points.

SUMMARY

In summary, relativistic electron beam generation via a capillary discharge guided LWFA was studied by using 15 mm long, 200 μm diameter and 33 mm long, 300 μm diameter capillary. Generation of quasi-monoenergetic e-beams up to 300 MeV was observed from the 15 mm long capillary, and up to 1 GeV was observed from the 33 mm long capillary. By using longer discharge delay, self-trapping was stabilized for the 15 mm long, 200 μm diameter capillary. This regime could be used to design a stable self injection capillary discharge guided LWFA. While reproducible beams have been observed in tightly controlled parameter regime, a controlled mechanism for injection will be important to enhance the LWFA performance.

ACKNOWLEDGMENTS

This work has been supported by the Director, Office of Science, High Energy Physics, U.S. Department of Energy under Contract No. DE-AC02-05CH11231 and DARPA. The authors acknowledge E. Cormier-Michel and E. Monaghan for their contributions.

REFERENCES

1. E. Esarey, et al., *IEEE Trans. Plasma Sci.* **24**, 252–288 (1996).
2. S. Mangles, et al., *Nature* **431**, 535–538 (2004).
3. C. G. R. Geddes, et al., *Nature* **431**, 538–541 (2004).
4. J. Faure, et al., *Nature* **431**, 541–544 (2004).
5. W. P. Leemans, et al., *Nature Physics* **2**, 696–699 (2006).
6. K. Nakamura, et al., *Physics of Plasmas* **14**, 056708 (2007).
7. A. J. Gonsalves, et al., *Physical Review Letters* **98**, 025002 (2007).
8. K. Nakamura, et al., *Rev. Sci. Instrum.* **79**, 053301 (2008).
9. A. J. Gonsalves, Ph.D. thesis, University of Oxford (2006).
10. T. P. Rowlands-Rees, et al., *Physical Review Letters* **100**, 105005 (2008).
11. C. D. Murphy, et al., *Physics of Plasmas* **13**, 033108 (2006).
12. E. Oz, et al., *Physical Review Letters* **98**, 084801 (2007).